International Journal of Pharmaceutics 550 (2018) 79–88

Contents lists available at ScienceDirect

International Journal of Pharmaceutics

journal homepage: www.elsevier.com/locate/ijpharm

Poly (L-glutamic acid)-g-methoxy poly (ethylene glycol)-gemcitabine conjugate improves the anticancer efficacy of gemcitabine

Chenguang Yang[a,b], Wantong Song[a], Dawei Zhang[a], Haiyang Yu[a], Lei Yin[c], Na Shen[a], Mingxiao Deng[d], Zhaohui Tang[a,*], Jingkai Gu[c,*], Xuesi Chen[a]

[a] Key Laboratory of Polymer Ecomaterials, Changchun Institute of Applied Chemistry, Chinese Academy of Sciences, Changchun 130022, PR China
[b] University of Chinese Academy of Sciences, Beijing 100039, PR China
[c] Research Center for Drug Metabolism, School of Life Sciences, Jilin University, Changchun, Jilin 130012, PR China
[d] College of Chemistry, Northeast Normal University, Changchun 130024, PR China

ARTICLE INFO

Keywords:
Gemcitabine
Nanoparticle
Pharmacokinetics
Biodistribution
Glutamic acid

ABSTRACT

Gemcitabine is widely used for anticancer therapy. However, its short blood circulation time and poor stability greatly impair its application. To solve this problem, we prepared a poly (L-glutamic acid)-g-methoxy poly (ethylene glycol)-gemcitabine conjugate (L-Gem) with a 14.3 wt% drug-loading content. L-Gem showed concentration- and time-dependent cytotoxicity towards 4T1, LLC, MIA PaCa-2 and A2780 *in vitro*. Pharmacokinetic and biodistribution studies indicated that L-Gem had remarkably enhanced blood stability, prolonged blood circulation time and greatly improved selective tumor distribution compared with free gemcitabine. The area under the concentration–time curve from zero to infinity [$AUC_{(0-\infty)}$] of L-Gem in plasma was 43-fold higher than that of free gemcitabine. The $AUC_{(0-\infty)}$ of the inactive metabolite, 2′-deoxy-2′,2′-difluorouridine in the L-Gem group was ~20% of that observed in the free gemcitabine group. The drug tumor accumulation ratio in the L-Gem group relative to the free gemcitabine group was 9.9 at 36 h, while the tumor AUC ratio was 15.8. Testing on Balb/C mice bearing the 4T1 tumor further demonstrated that L-Gem had significantly higher anticancer efficacy than free gemcitabine *in vivo*. These findings indicated that L-Gem has great potential for cancer treatment.

1. Introduction

Gemcitabine (dFdC), a deoxycytidine antimetabolite (Hingorani et al., 2016), is used against a wide range of solid tumors including those involving the pancreas (Dimcevski et al., 2016; Hessmann et al., 2017; Manji et al., 2017), breast, lung (non-small cell) (Hirsch et al., 2016), ovary and bladder (Heinemann, 2001; Reid et al., 2004). However, the plasma half-life of gemcitabine following intravenous administration is very short, at 8–17 min in humans (Abbruzzese et al., 1991b; Reid et al., 2004) and 9 min in mice (Moog et al., 2002). In addition, gemcitabine is unstable in blood (Croissant et al., 2016), with more than 91% metabolized directly to inactive 2′-deoxy-2′,2′-difluorouridine (dFdU) by deoxycytidine kinase and cytidine deaminase (Bouffard et al., 1993). This rapid inactivation significantly impairs the anticancer efficacy of gemcitabine (Richards et al., 2017). Indeed, high doses of gemcitabine are necessary to obtain a desired therapeutic response (Bastiancich et al., 2017). However, this simultaneously results in a variety of serious side effects such as myelosuppression, vomiting and nausea, elevated transaminases, hair loss, and hematuria and proteinuria (Abbruzzese et al., 1991a; Reddy et al., 2008). Therefore, it is important to prolong the blood circulation time of gemcitabine and improve its stability in the blood circulation system (Han et al., 2016; Liu et al., 2016).

To overcome these deficiencies in gemcitabine pharmacokinetics, several delivery systems have been developed. Two research groups have described PEG–gemcitabine prodrugs with significantly prolonged blood circulation time (Pasut et al., 2008; Vandana and Sahoo, 2010). PEGylation markedly improved the cytotoxicity and apoptosis-inducing activity of gemcitabine against pancreatic cancer cell lines (MIA PaCa 2 and PANC 1) (Jaidev et al., 2017). However, the low drug loading content of the PEG–gemcitabine prodrugs (0.98–6.39 wt%) limited their clinical applicability. Kiew et al. (2012, 2010) described a poly-L-glutamic acid-gemcitabine conjugate with dose-dependent cytotoxicity in several cancer cell lines and remarkable antitumor efficacy (Kiew et al., 2012). However, the stability and long blood circulation time of this conjugate have not been confirmed by pharmacokinetic and tissue

* Corresponding authors.
E-mail addresses: ztang@ciac.ac.cn (Z. Tang), gujk@mail.jlu.edu.cn (J. Gu).

https://doi.org/10.1016/j.ijpharm.2018.08.037
Received 11 March 2018; Received in revised form 28 July 2018; Accepted 18 August 2018
Available online 20 August 2018

distribution studies *in vivo*. Another approach to improve the biopharmaceutical properties of gemcitabine is to covalently couple its 4-amino group to squalenoyl to produce gemcitabine-squalene (Réjiba et al., 2011). Squalene is abundant in nature and well-tolerated after intravenous and oral administration (Reddy and Couvreur, 2009). Conjugation with squalene could protect the nucleoside of gemcitabine from the deamination process (Castelli et al., 2006). The gemcitabine-squalene conjugate (SQdFdC) has been shown to have greater anticancer efficacy than gemcitabine, when administered in an identical dosing schedule (Fiorini et al., 2015). However, the plasma area under the concentration-time curve (AUC) of dFdU in SQdFdC-treated mice was 2-fold greater than in the free gemcitabine group (Reddy et al., 2008). This indicated that SQdFdC stability in blood could be improved further.

Recently, we developed poly (L-glutamic acid)-graft-methoxy poly (ethylene glycol) (PLG-*g*-mPEG) as a nanocarrier for delivery of cisplatin, patupilone and combretastatin A4 (Liu et al., 2017; Shi et al., 2015; Song et al., 2016a, 2016b; Yan et al., 2017; Yu et al., 2016, 2015). Considering that PLG-*g*-mPEG has poly (L-glutamic acid) and poly (ethylene glycol) segments, it is rational to make a gemcitabine-PLG-*g*-mPEG conjugate (L-Gem). The PEG segments could give the obtained conjugate superior water solubility and longevity in blood circulation. The poly (L-glutamic acid) segments could graft a large amount of gemcitabine by covalently coupling carboxyl to the 4-amino group of gemcitabine. This could enable the conjugate to have high drug loading content, improved blood stability and long blood circulation time (Garrido-Laguna and Hidalgo, 2015; Li et al., 2016).

Thus, we prepared L-Gem and evaluated its use for cancer treatment. The drug release profile, cytotoxicity, pharmacokinetics and biodistribution of L-Gem were assessed and compared with free gemcitabine. The metabolic kinetics to produce dFdU from L-Gem and free gemcitabine were also investigated and compared.

2. Materials and methods

2.1. Materials

PLG-*g*-mPEG, with an average of 160 L-glutamic acid repeating units and 8.3 mPEG5K chains, was synthesized as described previously (Yu et al., 2015). Gemcitabine was purchased from Yangzhou Huihong Chemical Co. Ltd., China. N,N′-dimethylformamide (DMF) was stored over CaH_2 for 3 days and distilled under vacuum prior to use. N-hydroxysuccinimide (NHS) and 1-(3-dimethylaminopropyl)-3 ethylcarbodiimide hydrochloride (EDC·HCl) were supplied by Aladdin Reagent Co., Ltd., China. All other reagents and solvents were purchased from Sinopharm Chemical Reagent Co. Ltd., China and used as received.

2.2. Characterizations

Proton nuclear magnetic resonance (^{1}H NMR) spectra were recorded on an AV-300 or AV-400 spectrometer (Bruker, Germany) in trifluoroacetic acid-d or a sodium deuteroxide/deuterium oxide solution at room temperature. Gel permeation chromatography (GPC) measurements were conducted on a water GPC system (Waters Ultrahydrogel Linear column, 1515 HPLC pump with 2414 Refractive Index detector) using phosphate buffer (0.2 M, pH 7.4) as eluent (flow rate: 1 mL/min, 25 °C, and polyethylene glycol as the standard). Dynamic laser scattering (DLS) measurements were performed on a Wyatt QELS instrument with a vertically polarized He–Ne laser (DAWN EOS, Wyatt Technology, USA). The scattering angle was fixed at 90°. High performance liquid chromatography-mass spectrometry (HPLC-MS) was performed on a Triple TOF 5600 mass spectrometer with electrospray ionization source, Analyst TF data processing software, Agilent 1100 liquid chromatography system, and Shimadzu UFLC SIL-20A XR column compartment.

2.3. Preparation of L-Gem

L-Gem was synthesized through amidation between PLG-*g*-mPEG and gemcitabine in the presence of NHS and EDC·HCl. In brief, 500 mg of PLG-*g*-mPEG was dissolved in 10 mL of DMF. The temperature was kept at 0 °C and 1.5 mmol (175 mg) of NHS was added to the solution. The mixture was gradually brought to room temperature and stirred overnight. EDC·HCl [1.5 mmol (291 mg) dissolved in 5.0 mL DMF], gemcitabine [1 mmol (263 mg)] and triethylamine [1.5 mmol (154 mg) dissolved in 5.0 mL DMF] were then added into the reaction mixture. The mixture was then stirred at 50 °C under nitrogen protection. After 72 h, the reaction mixture was precipitated into excess cold ether to give the crude product, which was dissolved in phosphate buffer solution (pH 6.8) and dialysed against deionized water for 72 h (MWCO = 7000 Da). L-Gem was obtained after freeze-drying.

For evaluating the loading content and efficiency of gemcitabine, 10 mg L-Gem was dissolved in 10 mL NaOH solution (4 mg/mL) for 4 h. The concentration of gemcitabine released was measured by HPLC at 273 nm. Drug loading content (DLC) and drug loading efficiency (DLE) were calculated according to the following formulae:

$$\text{DLC (wt\%)} = (\text{weight of loaded gemcitabine}/\text{weight of L - Gem}) \times 100\%$$

$$\text{DLC (wt\%)} = (\text{weight of loaded gemcitabine} / \text{weight of feeding gemcitabine}) \times 100\%$$

2.4. Cell cultures

Murine breast cancer cells (4T1), Lewis lung cancer cells (LLC), human pancreatic carcinoma cells (MIA PaCa-2) and human ovarian carcinoma cells (A2780) were cultured at 37 °C in a 5% CO_2 atmosphere. Dulbecco's modified Eagle's medium (DMEM, Gibco, USA) supplemented with 10% fetal bovine serum, penicillin (50 U mL^{-1}) and streptomycin (50 U mL^{-1}) was used as the culture medium.

2.5. Animals

Balb/C mice (female, average body weight 18 g, 6–8 weeks old) and Sprague Dawley (SD) rats (male, average body weight 250 g) were obtained from Beijing Huafukang Biological Technology Co. Ltd. (HFK Bioscience, China). All animals received care in compliance with the guidelines outlined in the Guide for the Care and Use of Laboratory Animals and all procedures were approved by the Animal Care and Use Committee of Jilin University.

2.6. Drug release in vitro

The release of gemcitabine from L-Gem in phosphate-buffered saline (PBS) (pH 7.4 or 5.5) was evaluated by dialysis. Typically, 5.0 mg of L-Gem in 5 mL of PBS (pH 7.4 or 5.5) was added to a dialysis tube (MWCO 7000 Da), which was then incubated in 40 mL PBS buffer (pH 7.4 or 5.5) at 37 °C with a shaking rate of 100 rpm. At selected time intervals, 2 mL of incubated solution was taken out and replaced with an equal volume of fresh media.

The release of gemcitabine from L-Gem in Chym opapain b was also evaluated by dialysis. L-Gem 5.0 mg in 5 mL of water containing 0.2 mg Chym opapain b (800 U) was added to a dialysis tube (MWCO 7000 Da) (Zhang et al., 2017), which was then incubated in 40 mL PBS (pH 7.4) at 37 °C with a shaking rate of 100 rpm. At selected time intervals, 2 mL of incubated solution was taken out and replaced with an equal volume of fresh media.

Gemcitabine content was determined by HPLC. The HPLC system consisted of a reverse-phase C-18 column (Symmetry), with a mobile phase of acetonitrile and water (80:20 v/v) pumped at a flow rate of 1.0 mL/min at 25 °C. The column effluent was detected at 273 nm with

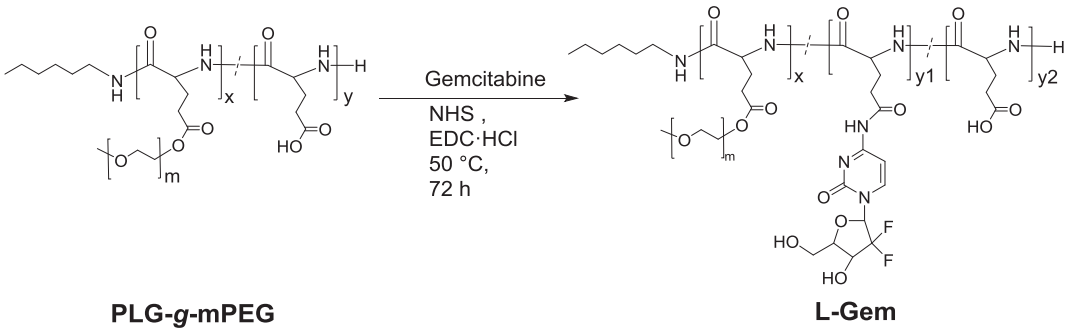

Scheme 1. Preparation of PLG-*g*-mPEG.

a UV detector (Waters 2489, USA).

2.7. MTT assay

4T1, LLC, MIA PaCa-2 or A2780 cells were seeded in 96-well plates with 6.0×10^3 cells per well in 180 μL of complete DMEM containing 10% fetal bovine serum supplemented with 50 U mL^{-1} penicillin and 50 U mL^{-1} streptomycin, and incubated at 37 °C in 5% CO_2 atmosphere for 24 h. The culture medium was replaced with 180 μL of fresh medium containing free gemcitabine and L-Gem at different concentrations. After 72 h incubation, 20 μL of MTT solution (5 mg mL^{-1} in PBS) was added into each well. With incubation for an additional 4 h, all 200 μL of solution was withdrawn and replaced with 150 μL DMSO. Solution absorbance was measured with a Bio-Rad 680 microplate reader at 490 nm. Cell viability (%) was calculated based on the following equation:

$$\text{Cell viability}\,(\%) = (A_{sample}/A_{control}) \times 100\%$$

where A_{sample} and $A_{control}$ represented the absorbance of the sample and control wells, respectively.

2.8. Pharmacokinetics

SD rats were randomly divided into two groups (n = 3, weight as mean ± SD: 250 ± 5 g). Gemcitabine or L-Gem was administered intravenously via the tail vein (4.0 mg/kg on a gemcitabine basis). At predefined time points (5, 15 and 45 min, and then 1, 1.5, 2, 4, 6, 9, 24 and 36 h), blood samples (500 μL) were collected from the orbital cavity, heparinized and centrifuged (15,000 rpm, 5 min) to obtain plasma.

Plasma L-Gem concentrations were determined using LC-MS/MS coupled with In-quadrupole CID. L-Gem underwent dissociation in the second quadrupole of mass spectrometer to generate gemcitabine related ions at *m/z* 112.0514. L-Gem was detected by positive ion electrospray ionization followed by high resolution extracted ions at *m/z* 112.0514. Dansyl chloride was used to derive gemcitabine and dFdU by decreasing their polarity and improving their chromatographic retention on the reversed-phase chromatographic column. After derivatisation, the MRM transitions of *m/z* 497.1 → 112.0, *m/z* 498.2 → 113.0 were chosen for the dansyl derivatives of gemcitabine and dFdU, respectively. Drug Statistics (DAS 3) software was used for data processing.

2.9. Biodistribution

BALB/c mice (n = 4, average body weight 18 g, 7 weeks old) were inoculated subcutaneously on the right flank with 4T1 mammary carcinoma cells (1×10^6). After 14 days, gemcitabine or L-Gem was administered intravenously at a dose of 2.8 mg/kg on a gemcitabine basis (mean ± SD tumor weight: 0.2 ± 0.05 g). The mice were sacrificed at predefined periods (3, 12, 24 and 36 h), and the tumor, brain, heart, kidneys, liver, spleen, lungs and gastric wall were excised. The tissues were rinsed with physiological saline, wiped dry with filter paper and the weight recorded. Tissue collection and homogenization were performed at 0–4 °C. The tissue was cut into small pieces, with 2.0 mL of methanol/water (1:1, v/v) solution added per 1.0 g of tissue. After homogenization for 15 s, the mixture was centrifuged (4500 rpm) for 10 min. The supernatant was collected and stored at −80 °C until tested. The concentration of gemcitabine, L-Gem and dFdU in the solution was measured by LC-MS/MS.

2.10. Antitumor efficacy in vivo

4T1 tumor model was generated by injecting subcutaneously 4T1 cells (1×10^6) into the mammary fat pads of Balb/C mice (Song et al., 2016c). At a tumor volume of approximately 50 mm^3, the mice were randomly divided into six groups (n = 8 each) and treated twice with PBS (pH = 7.4, 0.2 mL), gemcitabine (40 or 200 mg/kg, 0.2 mL) or L-Gem (20, 30 or 40.0 mg/kg on a gemcitabine basis, 0.2 mL) by intravenous injection on days 0 and 7. Tumor volume and body weight were used to assess treatment efficacy and systemic toxicity, respectively. Tumor volume was calculated using the following formula:

$$\text{Tumor volume}\,(V) = a \times b^2/2$$

Where a and b were the longest and shortest tumor diameters measured with vernier calipers.

2.11. Confocal laser scanning microscopy (CLSM) observation

The cellular uptake behavior of dihydrorhodamine 123-labeled L-Gem was investigated in 4T1 cells using CLSM. The cells were seeded on the coverslips of 6-well plates (1×10^5 cells per well), and incubated for 24 h. The original medium was then replaced with fresh DMEM containing dihydrorhodamine 123-labeled L-Gem micelles, which was removed after 1, 2 or 6 h incubation. The cells were washed with PBS and fixed with PBS containing 4% formaldehyde at room temperature for 20 min before staining the cell nuclei with 4′,6-diamidino-2-phenylindole (DAPI). The coverslips were placed onto glass microscope slides. Dihydrorhodamine 123-labeled L-Gem uptake by B16F1 cells was observed using a laser scanning confocal microscope (Carl Zeiss LSM 700, Germany).

2.12. Data analysis

All experiments were performed at least three times and expressed as means ± SD. The data were analyzed for statistical significance using one-way ANOVA, with $p < 0.05$ considered statistically significant, $p < 0.01$ considered highly significant, and $p < 0.001$ considered extremely significant.

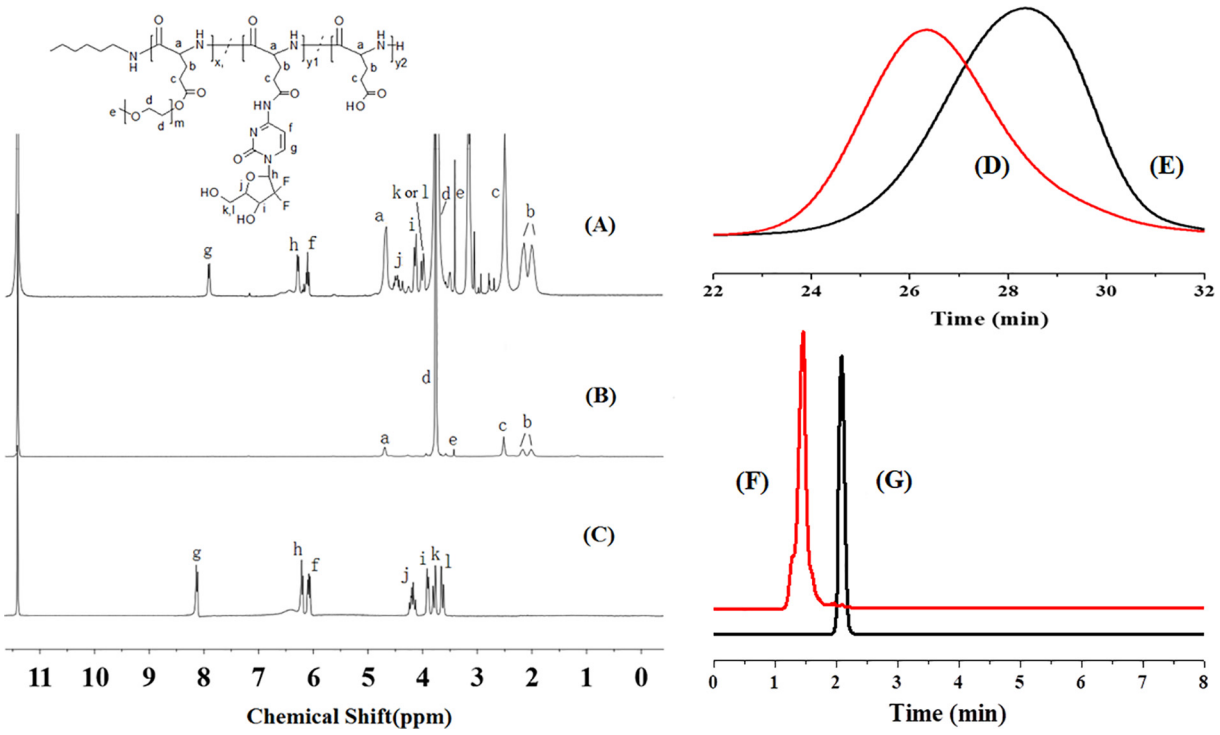

Fig. 1. ^{1}H NMR spectra of (A) L-Gem, (B) PLG-*g*-mPEG and (C) gemcitabine in CF_3COOD. GPC spectra of L-Gem (D) and PLG-g-mPEG (E). HPLC spectra of L-Gem (F) and gemcitabine (G).

3. Results and discussion

3.1. Preparation of L-Gem

PLG-*g*-mPEG is a biodegradable polymeric carrier where the mPEG segments are conjugated to glutamic acid units by ester bonds. It can significantly prolong the blood circulation time of drugs such as cisplatin, patupilone and combretastatin A4 (Li et al., 2015; Liu et al., 2017). For L-Gem preparation, the carboxyl groups of PLG-*g*-mPEG were activated by NHS, which were then conjugated to the amino groups of gemcitabine to form amide bonds in the presence of EDC (Scheme 1). The ^{1}H NMR spectra of L-Gem and gemcitabine in CF_3COOD are shown in Fig. 1. The appearance of the characteristic peaks, h (furan protons of gemcitabine, δ 6.40 ppm), and g and f (pyrimidine protons of gemcitabine, δ 8.11 ppm and δ 6.10 ppm) in the ^{1}H NMR spectrum of L-Gem (Fig. 1A) indicated that gemcitabine was successfully grafted to the PLG-*g*-mPEG.

The GPC curves of PLG-*g*-mPEG and L-Gem had single peaks (Fig. 1). PLG-*g*-mPEG had a M_n of 31.2×10^3 g mol^{-1} and polydispersity index (PDI) of 1.37, whereas for L-Gem the values were 36.1×10^3 g mol^{-1} and 1.39, respectively. HPLC indicated that the DLC of L-Gem was 14.3 wt%, while the DLE was 51.2%. ^{1}H NMR indicated that the DLC of L-Gem was 13.9 wt%, and the DLE was 49.8%. Thus, the HPLC and ^{1}H NMR findings were consistent.

HPLC curves of L-Gem (A) and gemcitabine (B) are shown in Fig. 1. The mobile phase was acetonitrile and water (v1/v2 = 4:1). The measurement wavelength was 267 nm. The PLG-*g*-mPEG peak was at 1.48 min (A) and the gemcitabine peak was at 2.11 min (B). In Fig. 1F, the gemcitabine signal did not appear in the spectrum of L-Gem, which indicated that L-Gem was prepared successfully without residual free gemcitabine (Bastiancich et al., 2016).

As an amphiphilic polymer, L-Gem can self-assemble into micelles in

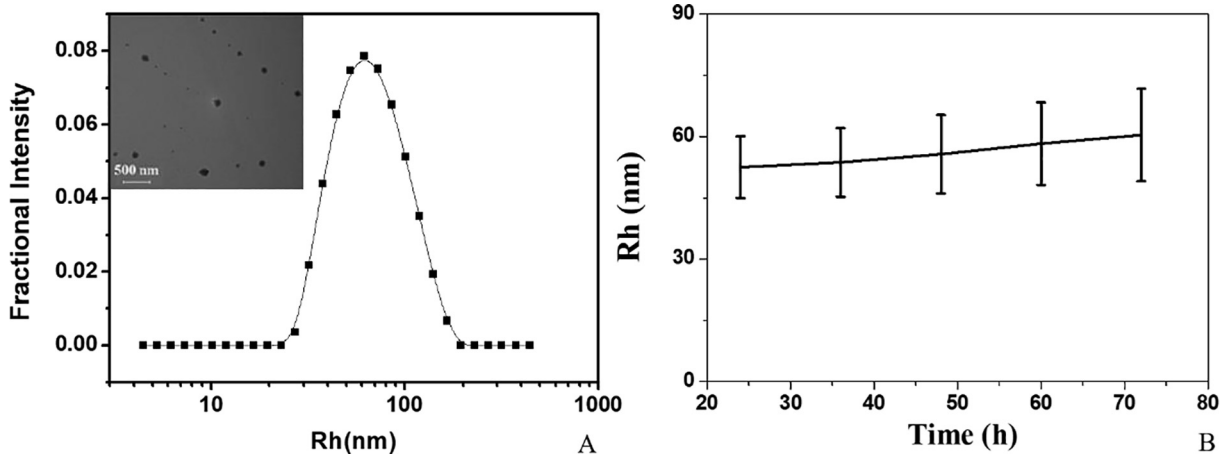

Fig. 2. Hydrodynamic radius distribution and typical morphology of L-Gem in aqueous solution estimated by DLS and TEM, respectively (A). Stability of L-Gem in PBS (pH 7.4) estimated by DLS (B).

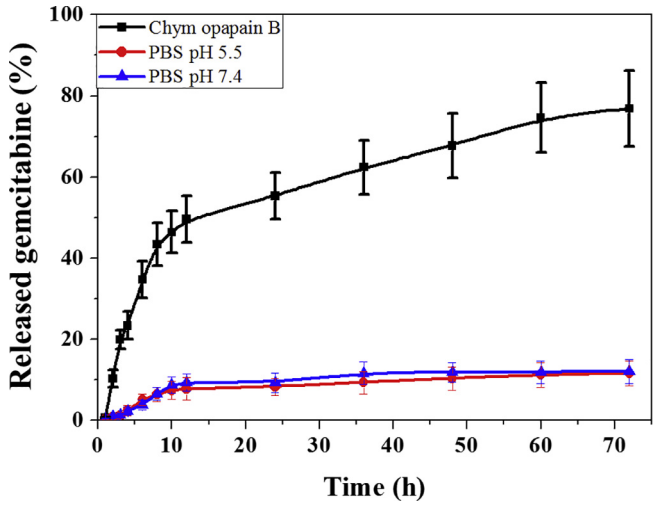

Fig. 3. Release profiles of L-Gem in PBS at pH 5.5, in PBS at pH 7.4, or in PBS at pH 7.4 with 0.04 mg/mL Chym opapain b solution (800 U). The data are presented as mean ± SD (n = 3).

aqueous solution. The hydrodynamic radius (R_h) of L-Gem micelles measured by DLS was 52.4 ± 18.3 nm, and the diameter determined by TEM was 78.6 ± 27 nm (Fig. 2A). L-Gem micelles were stable in PBS at pH 7.4 (Fig. 2B). After intravenous administration, nanoparticles that are approximately 100 nm in diameter can be retained in the blood circulation and accumulate in solid tumors, via the leaky vasculature, by the enhanced permeability and retention (EPR) effect (< 400 nm) (King and Dedrick, 1992; Maeda et al., 2000). This indicates that L-Gem has a great potential to passively target to solid tumors.

3.2. Drug release in vitro

The *in vitro* release profiles of L-Gem in PBS (pH 7.4 or 5.5) at 37 °C are shown in Fig. 3. After 72 h, less than 15% of gemcitabine was released from L-Gem at either pH value, indicating that L-Gem was relatively stable in an environment lacking enzymes. The gemcitabine moieties were conjugated to PLG-*g*-mPEG via amide bonds that could be cleaved by protease such as Chym opapain b. In the presence of Chym opapain b, 77% of gemcitabine was released from L-Gem after 72 h indicating that gemcitabine could be efficiently liberated from L-Gem by enzymes *in vivo*.

3.3. Cytotoxicity assay in vitro

Gemcitabine and L-Gem cytotoxicities were evaluated by MTT assay in various cell types (4T1, LLC, MIA PaCa-2 and A2780). As shown in Fig. 4, both gemcitabine and L-Gem showed dose- and time-dependent inhibition of cell proliferation. In addition, cell viability for both gemcitabine and L-Gem at 72 h was lower than at 48 h for all four cell lines. IC_{50} values are listed in Table 1. These showed that L-Gem had slightly lower cytotoxicity than free gemcitabine, which is reasonable because L-Gem is a prodrug for gemcitabine.

3.4. Plasma pharmacokinetics and biodistribution

Plasma pharmacokinetics studies for gemcitabine and L-Gem were conducted *in vivo* using SD rats. Gemcitabine and L-Gem were administered intravenously via the tail vein. As shown in Fig. 5A, gemcitabine was cleared rapidly from the blood circulation or transformed into other forms. Compared with the plasma gemcitabine concentration at 5 min post-dose, gemcitabine concentrations were only 9.97%, 2.02% and 1.63% at 6, 24 and 36 h. In contrast, L-Gem concentrations at 6, 24 and 36 h were 57.2%, 42.2% and 37.1% of those achieved at 5 min. Plasma pharmacokinetic parameters are shown in Table 2. The AUC for L-Gem in plasma was 43-fold higher than for free gemcitabine. The half-lives were 6.41 h for L-Gem versus 40.02 min for free gemcitabine. These indicated that L-Gem possessed a remarkably prolonged blood circulation time compared with free gemcitabine. As shown in Fig. 5B, plasma exposure to gemcitabine in the L-Gem group was far lower than in the gemcitabine group. Consistently, plasma dFdU concentrations in the L-Gem group were far lower than in the gemcitabine group (Fig. 5C). The AUC of dFdU in the L-Gem group was approximately 20% of that in the gemcitabine group (2628 ± 692 versus 13,359 ± 1928 μg × h/L) (Table 2). Collectively, these findings suggested that blood stability had been improved significantly with L-Gem (Yang et al., 2015).

Biodistribution studies were conducted *in vivo* in Balb/c mice bearing 4T1 tumors. The distribution of gemcitabine and L-Gem in the heart, liver, spleen, brain, lung, gastric wall, kidney and 4T1 solid tumors are shown in Fig. 6. The gemcitabine tumor concentration (Fig. 6A) was 42.6 μg/g at 3 h post-injection of free gemcitabine, and then quickly dropped to 10.4 μg/g at 12 h. dFdU was detected at a very high concentration of 4351.7 μg/g (Fig. 6B) at 3 h. As all dFdU must come from gemcitabine, it is clear that most free gemcitabine was metabolised rapidly to inactive dFdU in the free gemcitabine group. In contrast, after injection of L-Gem, there was 220.5 μg/g gemcitabine (Fig. 6C) in the form of L-Gem in the tumor at 3 h (75.3 μg/g at 12 h, 39.7 μg/g at 24 h and 23.4 μg/g at 36 h) and 110.0 μg/g gemcitabine (Fig. 6D) in the form of free gemcitabine. Further, the tumor concentration of dFdU was 668.1 μg/g (Fig. 6E) at 3 h after L-Gem injection. The significantly lower tumor dFdU concentration in the L-Gem group compared with the free gemcitabine group (Fig. 6F) is likely due to PLG-*g*-mPEG protecting gemcitabine.

After injection of free gemcitabine, its concentration in the spleen was 256.9 μg/g at 3 h and then quickly reduced to 39.2 μg/g at 12 h. Liver and kidney concentrations of gemcitabine were very low. The concentration of dFdU in the spleen was 726.9 μg/g at 3 h, and 391.1 μg/g at 12 h. Kidney concentrations of dFdU were higher at 4266.1 μg/g at 3 h, and 1051.9 μg/g at 12 h. These findings indicated that gemcitabine was highly metabolized in the spleen, and excreted through the kidneys as dFdU.

After injection of L-Gem, the liver had the highest drug concentration (414.0 μg/g at 3 h and 380.1 μg/g at 24 h). Hepatic metabolism of L-Gem to dFdU (11.5 μg/g at 3 h) occurred at a much slower rate than with free gemcitabine due to the protection of gemcitabine by PLG-*g*-mPEG. This will improve the anticancer efficacy (Park et al., 2015).

The ratios of gemcitabine accumulation and AUC in 4T1 tumors versus normal tissues 36 h after intravenous administration of gemcitabine or L-Gem are summarized in Table 3. The AUC was calculated according to the trapezoidal rule up to 36 h. The drug accumulation ratio of tumor to brain tissue was 2.64 in the gemcitabine group, and 15.19 in the L-Gem group. For tumor to gastric wall and spleen tissue, the drug accumulation ratios in the gemcitabine group were 0.53 and 0.23, respectively. These ratios were higher in the L-Gem group at 2.03 and 0.85, respectively. The drug tumor accumulation ratio of the L-Gem group relative to the free gemcitabine group was 9.9. The AUC ratio of tumor to brain tissue increased from 2.01 for the free gemcitabine group to 27.97 for the L-Gem group. The AUC ratio of tumor to gastric wall tissue increased from 0.58 in the gemcitabine group to 1.01 in the L-Gem group. The total drug AUC ratio of tumor to spleen increased from 0.28 in the gemcitabine group to 1.63 in the L-Gem group. The tumor AUC ratio of the L-Gem group relative to the free gemcitabine group was 15.8. All these data suggested that L-Gem greatly improved selective distribution of gemcitabine into tumors due to enhanced stability and prolonged blood circulation time (Goji et al., 2015).

3.5. Anticancer efficacy of gemcitabine and L-Gem in vivo

The anti-tumor efficacy was tested *in vivo* on Balb/C mice bearing

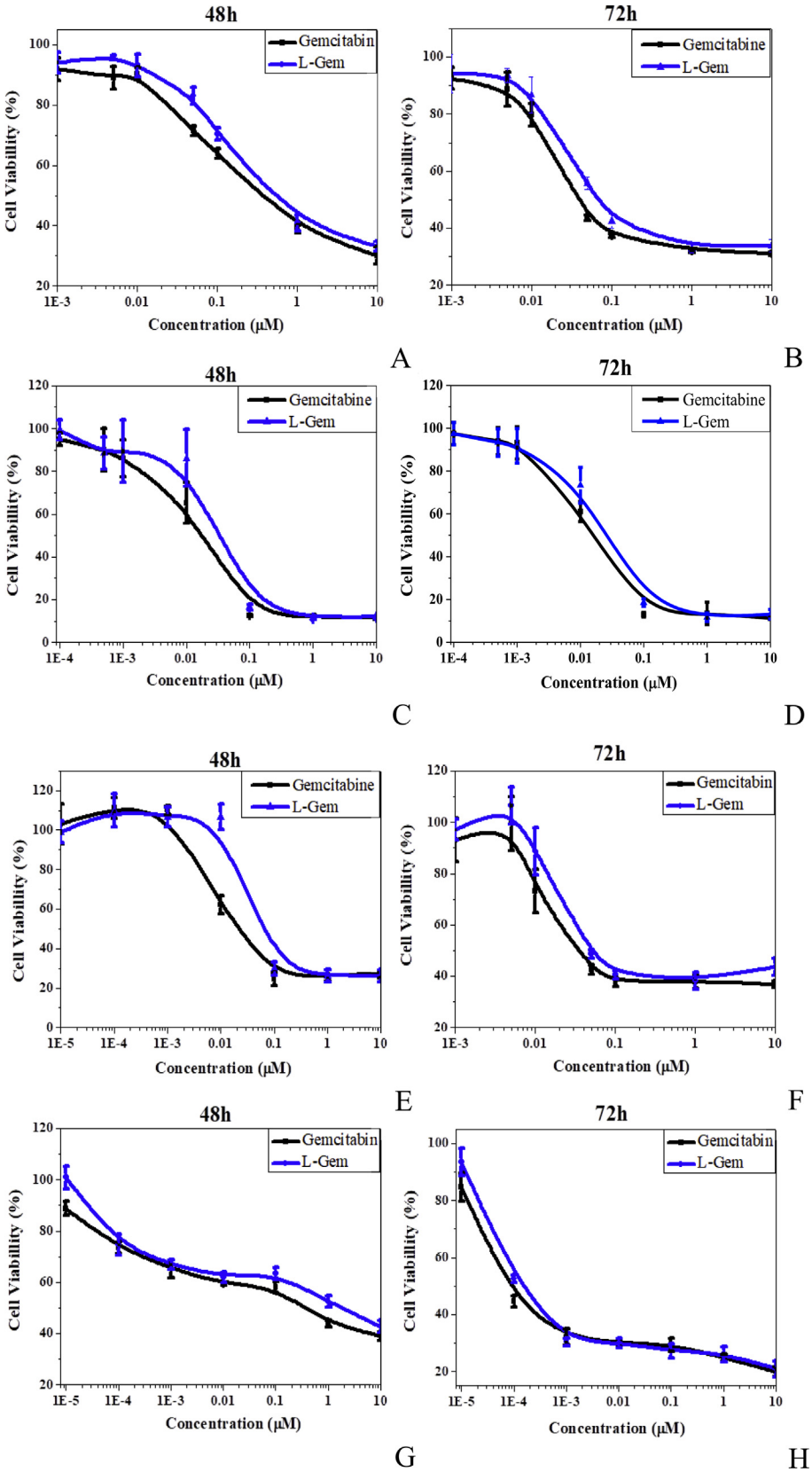

Fig. 4. Cytotoxicities of gemcitabine or L-Gem *in vitro* against 4T1for 48 h (A) and 72 h (B), LLC for 48 h (C) and 72 h (D), MIA PaCa-2 cells for 48 h (E) and 72 h (F), and A2780 for 48 h (G) and 72 h (H).

Table 1
Gemcitabine and L-Gem IC_{50} values after incubation times of 48 or 72 h.

	IC_{50} (μM)			
Incubation time (h)	48 h	48 h	72 h	72 h
Cell line	Gemcitabine	L-Gem	Gemcitabine	L-Gem
4T1	0.186	0.352	0.037	0.069
LLC	0.057	0.074	0.051	0.068
Mia PaCa-2	0.022	0.065	0.007	0.015
A2780	0.279	1.629	8.29e-5	1.66e-4

Table 2
Plasma pharmacokinetic parameters of gemcitabine, L-Gem and dFdU after a single intravenous administration of gemcitabine and L-Gem.

Injection form	Drugs	$AUC_{(0-\infty)}$ [a] (μg × h/L)	C_{max} [b] (μg/L)
Gemcitabine	Gem	138,291 ± 18,069	39,533 ± 5934
	dFdU	13,359 ± 1928	584.67 ± 262.71
L-Gem	L-Gem	6,070,403 ± 574,528	137,666 ± 4652
	Gem	51,476 ± 8793	4600 ± 1124
	dFdU	2628 ± 692	76.9 ± 36.5

[a] $AUC_{(0-\infty)}$: area under the drug concentration–time curve in plasma from zero to infinity.
[b] C_{max}: maximum concentration.

4T1 tumors. As shown in Fig. 7A, the tumor volume at day 18 in the gemcitabine 40 or 200 mg/kg, and L-Gem 20, 30 or 40 mg/kg treated groups were 77.6%, 56.2%, 60.0%, 43.3% and 30.3% of the PBS group, respectively. L-Gem 40 mg/kg had greater antitumor efficacy than free gemcitabine 200 mg/kg. L-Gem 20, 30 and 40 mg/kg showed higher anti-tumor efficacy than free gemcitabine 40 mg/kg. The improved anticancer efficacy of L-Gem was attributed to the enhanced selective tumor distribution of L-Gem compared with free gemcitabine. This was due to the improved stability and long blood circulation shown in the pharmacokinetic and biodistribution studies. The change in body weight of the treated groups was insignificant compared with the control group (Fig. 7B), indicating low systemic toxicity of L-Gem (Meng et al., 2016).

3.6. CLSM observation

Cellular uptake of L-Gem micelles were investigated in 4T1 cells using CLSM, with cell nuclei stained with DAPI (blue). L-Gem was labeled with dihydrorhodamine 123 (red) to investigate the subcellular location of these micelles qualitatively. Dihydrorhodamine 123 was conjugated to the remaining carboxyl groups of L-Gem. As shown in Fig. 8, after incubation with dihydrorhodamine 123-labeled L-Gem micelles for 1 and 2 h, the red fluorescence was observed in cell cytoplasm. After a 6 h incubation period, cellular uptake of L-Gem was improved and the red fluorescence was distributed more widely in the cytoplasm. This indicated that L-Gem micelle could be internalized by tumor cells.

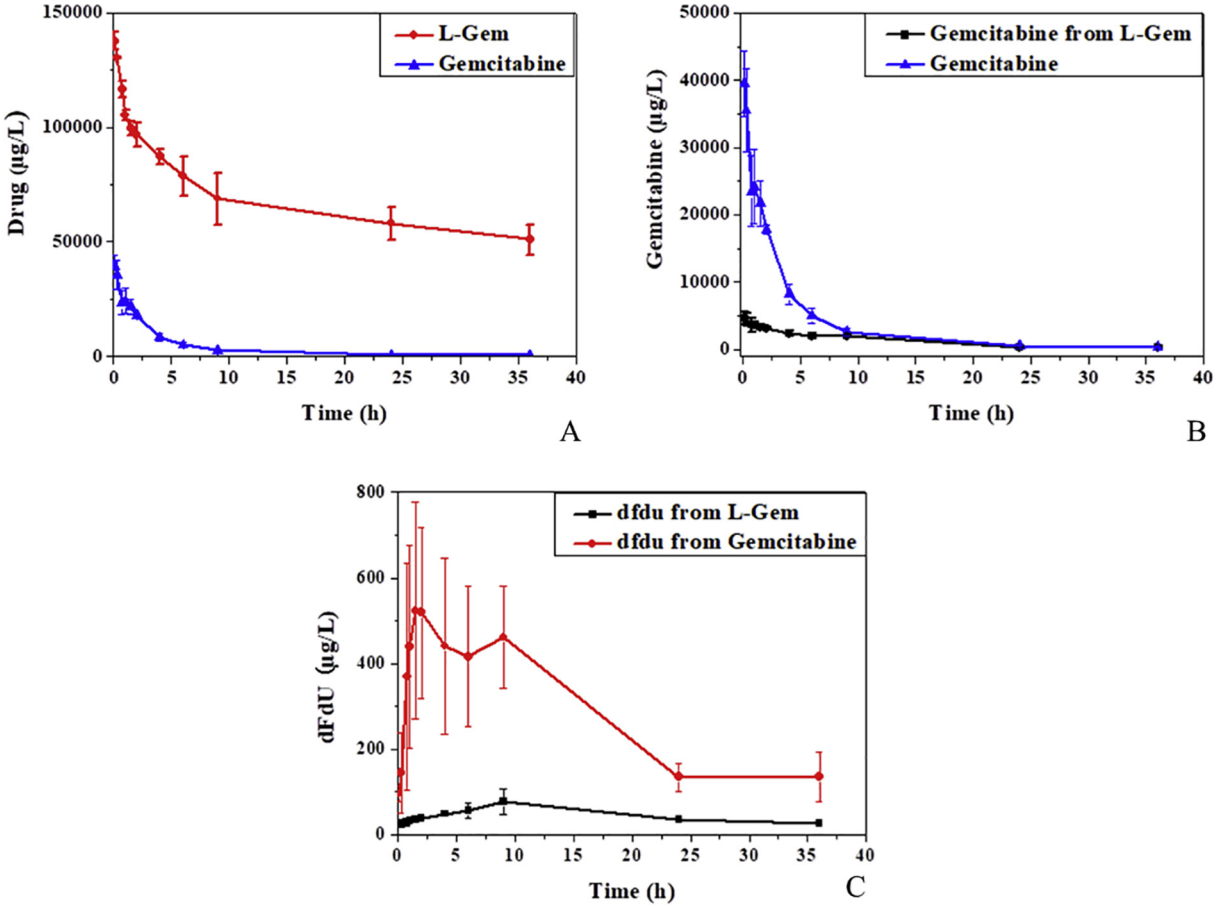

Fig. 5. Plasma concentration-time profiles of gemcitabine, L-Gem and dFdU after administration of gemcitabine and L-Gem to healthy rats at a dose of 4 mg/kg based on gemcitabine. Each group is expressed as mean ± SD (n = 3). (A) L-Gem and gemcitabine concentrations in rat plasma. (B) Gemcitabine concentrations rat plasma. (C) dFdU concentrations in rat plasma.

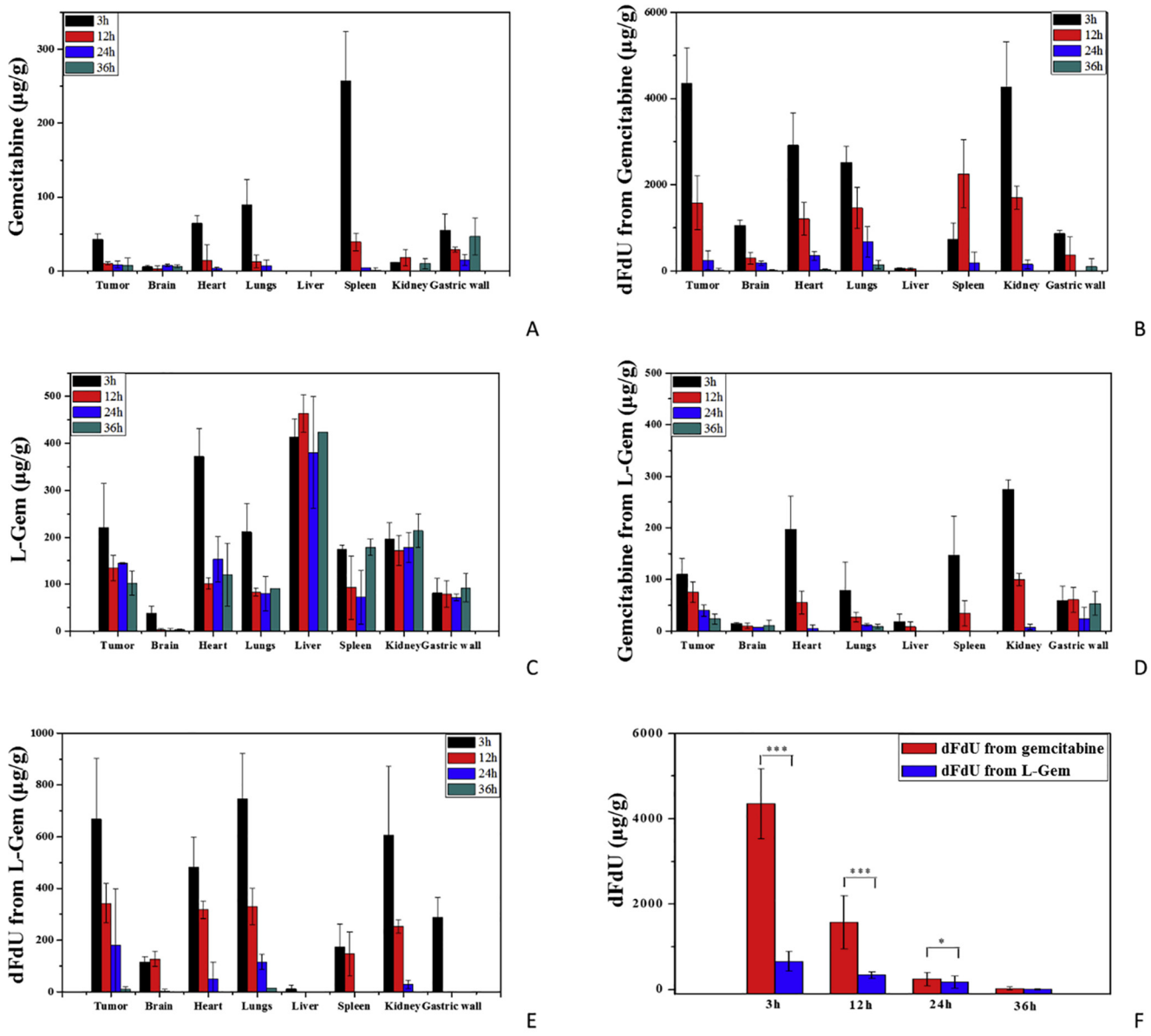

Fig. 6. Distribution of gemcitabine (A) and dFdU (B) after administration of gemcitabine. Distribution of L-Gem (C) (converted to gemcitabine content), gemcitabine (D) and dFdU (E) after administration of L-Gem. Statistical analysis of dFdU tumor distribution (F). Each drug was administered to female BALB/c mice at a dose of 2.8 mg/kg on a gemcitabine basis. Data are presented as the mean ± SD (n = 4). $^{*}P < 0.05$, $^{***}P < 0.001$.

Table 3
Accumulation ratios and area under the concentration-time curve (AUC) ratios between the tumor (4T1) and normal tissues 36 h after administration of free gemcitabine and L-Gem.[a]

	Accumulation ratio			AUC ratio[b]		
	Gem	Gem from L-Gem	L-Gem	Gem	Gem from L-Gem	L-Gem
Tumor/Brain	2.64	5.21	15.19	2.01	4.74	27.97
Tumor/Heart	2.00	0.94	0.85	2.24	1.15	1.00
Tumor/Lungs	1.99	1.83	1.37	1.63	2.06	1.45
Tumor/Liver	–	11.67	0.36	–	9.32	0.31
Tumor/Spleen	0.23	1.57	1.50	0.28	1.66	1.63
Tumor/Kidney	1.12	0.63	0.85	1.15	0.76	0.24
Tumor/Gastric wall	0.53	1.31	2.03	0.58	1.14	1.01

[a] Dose: 2.8 mg/kg on gemcitabine basis.
[b] AUC was calculated based on the trapezoidal rule up to 36 h.

4. Conclusions

In this work, L-Gem was successfully synthesized by conjugation of PLG-*g*-mPEG and gemcitabine. L-Gem showed a concentration- and time-dependent cytotoxicity towards a variety of cancer cell lines *in vitro*. L-Gem had remarkably improved blood stability and prolonged blood circulation time compared with free gemcitabine. The plasma $AUC_{(0-\infty)}$ of L-Gem was 43-fold higher than that of free gemcitabine. The $AUC_{(0-\infty)}$ of dFdU in the L-Gem group was ~20% of that observed in the free gemcitabine group. In addition, L-Gem had greatly improved selective tumor distribution. The drug tumor accumulation ratio of the L-Gem group relative to the free gemcitabine group was 9.9 at 36 h, whereas the tumor AUC ratio was 15.8. Further testing *in vivo* indicated that L-Gem had significantly greater anticancer efficacy than free gemcitabine. Therefore, L-Gem had improved stability and a longer half-life making it a potential drug candidate to replace gemcitabine for cancer treatment.

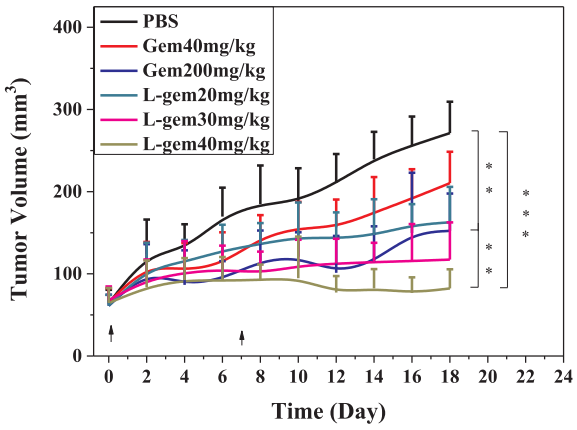

(A)

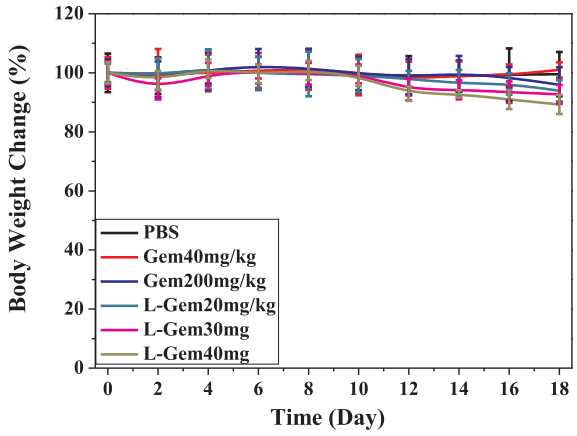

(B)

Fig. 7. Antitumor efficacy of gemcitabine and L-Gem *in vivo,* in the 4T1 tumor bearing mouse model. (A) Tumor volume changes; (B) Body weight relative to the start point as a function of time. Gemcitabine or L-Gem was injected twice on days 0 and 7. The data are shown as mean ± SD (n = 8), $^{**}P < 0.01$, $^{***}P < 0.001$.

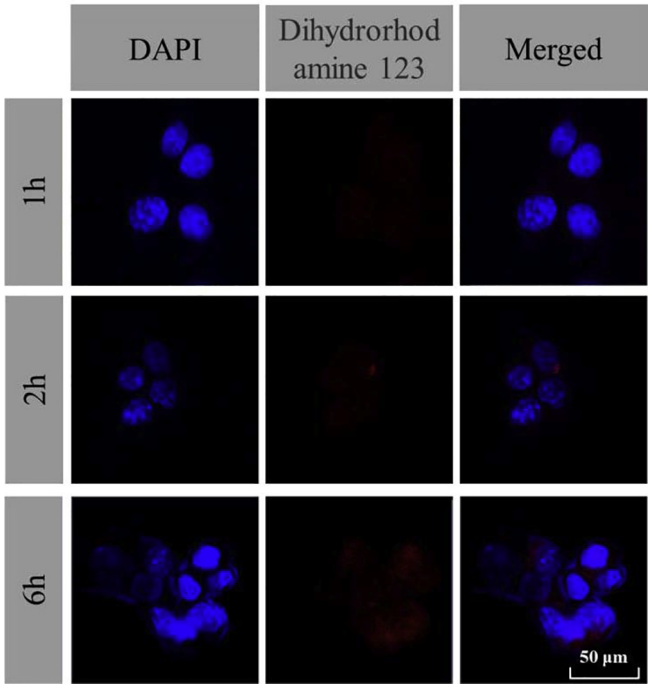

Fig. 8. Confocal laser scanning microscopy images of 4T1 cells after incubation with dihydrorhodamine 123-labeled L-Gem for 1, 2 and 6 h.

Acknowledgments

This work was financially supported by the National Natural Science Foundation of China (Projects 51390484, 51673189, 51673185, 51473029 and 81430087), the Ministry of Science and Technology of China (Project 2018ZX09711003-012), the Program of Scientific Development of Jilin Province (No. 20170101100JC) and the Chinese Academy of Sciences Youth Innovation Promotion Association.

Appendix A. Supplementary data

Supplementary data associated with this article can be found, in the online version, at https://doi.org/10.1016/j.ijpharm.2018.08.037.

References

Abbruzzese, J.L., Grunewald, R., Weeks, E.A., Gravel, D., Adams, T., Nowak, B., Mineishi, S., Tarassoff, P., Satterlee, W., Raber, M.N., 1991a. A phase I clinical, plasma, and cellular pharmacology study of gemcitabine. J. Clin. Oncol. 9, 491–498.

Abbruzzese, J.L., Grunewald, R., Weeks, E.A., Gravel, D., Adams, T., Nowak, B., Mineishi, S., Tarassoff, P., Satterlee, W., Raber, M.N., Plunkett, W., 1991b. A phase-I clinical, plasma, and cellular pharmacology study of gemcitabine. J. Clin. Oncol. 9, 491–498.

Bastiancich, C., Bianco, J., Vanvarenberg, K., Ucakar, B., Joudiou, N., Gallez, B., Bastiat, G., Lagarce, F., Preat, V., Danhier, F., 2017. Injectable nanomedicine hydrogel for local chemotherapy of glioblastoma after surgical resection. J. Control. Release 264, 45–54.

Bastiancich, C., Vanvarenberg, K., Ucakar, B., Pitorre, M., Bastiat, G., Lagarce, F., Preat, V., Danhier, F., 2016. Lauroyl-gemcitabine-loaded lipid nanocapsule hydrogel for the treatment of glioblastoma. J. Control. Release 225, 283–293.

Bouffard, D.Y., Laliberte, J., Momparler, R.L., 1993. Kinetic-studies on 2′,2′-difluorodeoxycytidine (gemcitabine) with purified human deoxycytidine kinase and cytidine deaminase. Biochem. Pharmacol. 45, 1857–1861.

Castelli, F., Sarpietro, M.G., Ceruti, M., Rocco, F., Cattel, L., 2006. Characterization of lipophilic gemcitabine prodrug - liposomal membrane interaction by differential scanning calorimetry. Mol. Pharm. 3, 737–744.

Croissant, J.G., Zhang, D.Y., Alsaiari, S., Lu, J., Deng, L., Tamanoi, F., AlMalik, A.M., Zink, J.I., Khashab, N.M., 2016. Protein-gold clusters-capped mesoporous silica nanoparticles for high drug loading, autonomous gemcitabine/doxorubicin co-delivery, and in-vivo tumor imaging. J. Control. Release 229, 183–191.

Dimcevski, G., Kotopoulis, S., Bjanes, T., Hoem, D., Schjott, J., Gjertsen, B.T., Biermann, M., Molven, A., Sorbye, H., McCormack, E., Postema, M., Gilja, O.H., 2016. A human clinical trial using ultrasound and microbubbles to enhance gemcitabine treatment of inoperable pancreatic cancer. J. Control. Release 243, 172–181.

Fiorini, C., Cordani, M., Gotte, G., Picone, D., Donadelli, M., 2015. Onconase induces autophagy sensitizing pancreatic cancer cells to gemcitabine and activates Akt/mTOR pathway in a ROS-dependent manner. Biochim. Biophys. Acta 1853, 549–560.

Garrido-Laguna, I., Hidalgo, M., 2015. Pancreatic cancer: from state-of-the-art treatments to promising novel therapies. Nat. Rev. Clin. Oncol. 12, 319–334.

Goji, T., Kimura, T., Miyamoto, H., Takehara, M., Kagemoto, K., Okada, Y., Okazaki, J., Takaoka, Y., Miyamoto, Y., Mitsui, Y., Matsumoto, S., Sueuchi, T., Tanaka, K., Fujino, Y., Takaoka, T., Kitamura, S., Okamoto, K., Kimura, M., Sogabe, M., Muguruma, N., Okahisa, T., Sato, Y., Sagawa, T., Fujikawa, K., Sato, Y., Ikushima, H., Takayama, T., 2015. A phase I/II study of fixed-dose-rate gemcitabine and S-1 with concurrent radiotherapy for locally advanced pancreatic cancer. Cancer Chemother. Pharmacol. 76, 615–620.

Han, H.J., Wang, H.B., Chen, Y.J., Li, Z.H., Wang, Y., Jin, Q., Ji, J., 2016. Theranostic reduction-sensitive gemcitabine prodrug micelles for near-infrared imaging and pancreatic cancer therapy. Nanoscale 8, 283–291.

Heinemann, V., 2001. Gemcitabine: progress in the treatment of pancreatic cancer. Oncology-Basel 60, 8–18.

Hessmann, E., Johnsen, S.A., Siveke, J.T., Ellenrieder, V., 2017. Epigenetic treatment of pancreatic cancer: is there a therapeutic perspective on the horizon? Gut 66, 168–179.

Hingorani, S.R., Harris, W.P., Beck, J.T., Berdov, B.A., Wagner, S.A., Pshevlotsky, E.M., Tjulandin, S.A., Gladkov, O.A., Holcombe, R.F., Korn, R., Raghunand, N., Dychter, S., Jiang, P., Shepard, H.M., Devoe, C.E., 2016. Phase Ib study of PEGylated recombinant human hyaluronidase and gemcitabine in patients with advanced pancreatic cancer. Clin. Cancer Res. 22, 2848–2854.

Hirsch, F.R., Suda, K., Wiens, J., Bunn, P.A., 2016. New and emerging targeted treatments in advanced non-small-cell lung cancer. Lancet 388, 1012–1024.

Jaidev, L.R., Chellappan, D.R., Bhaysar, D.V., Ranganathan, R., Sivanantham, B., Subramanian, A., Sharma, U., Jagannathan, N.R., Krishnan, U.M., Sethuraman, S., 2017. Multi-functional nanoparticles as theranostic agents for the treatment & imaging of pancreatic cancer. Acta Biomater. 49, 422–433.

Kiew, L.V., Cheong, S.K., Ramli, E., Sidik, K., Lim, T.M., Chung, L.Y., 2012. Efficacy of a poly-L-glutamic acid-gemcitabine conjugate in tumor-bearing mice. Drug Dev. Res. 73, 120–129.

Kiew, L.V., Cheong, S.K., Sidik, K., Chung, L.Y., 2010. Improved plasma stability and sustained release profile of gemcitabine via polypeptide conjugation. Int. J. Pharm. 391, 212–220.

King, F.G., Dedrick, R.L., 1992. Physiological pharmacokinetic parameters for cis-

dichlorodiammineplatinum(Ii) (Ddp) in the mouse. J. Pharmacokinet. Biopharm. 20, 95–99.
Li, L.L., Tong, R., Li, M.Y., Kohane, D.S., 2016. Self-assembled gemcitabine-gadolinium nanoparticles for magnetic resonance imaging and cancer therapy. Acta Biomater. 33, 34–39.
Li, Y.F., Yu, H.Y., Sun, H., Liu, J.G., Tang, Z.H., Wang, D., Yu, L.Y., Chen, X.S., 2015. Cisplatin-loaded poly(L-glutamic acid)-g-Methoxy poly(ethylene glycol) nanoparticles as a potential chemotherapeutic agent against osteosarcoma. Chin. J. Polym. Sci. 33, 763–771.
Liu, T., Zhang, D., Song, W., Tang, Z., Zhu, J., Ma, Z., Wang, X., Chen, X., Tong, T., 2017. A poly(L-glutamic acid)-combretastatin A4 conjugate for solid tumor therapy: markedly improved therapeutic efficiency through its low tissue penetration in solid tumor. Acta Biomater. 53, 179–189.
Liu, X.S., Situ, A., Kang, Y.A., Villabroza, K.R., Liao, Y.P., Chang, C.H., Donahue, T., Nel, A.E., Meng, H., 2016. Irinotecan delivery by lipid-coated mesoporous silica nanoparticles shows improved efficacy and safety over liposomes for pancreatic cancer. ACS Nano 10, 2702–2715.
Maeda, H., Wu, J., Sawa, T., Matsumura, Y., Hori, K., 2000. Tumor vascular permeability and the EPR effect in macromolecular therapeutics: a review. J. Control. Release 65, 271–284.
Manji, G.A., Olive, K.P., Saenger, Y.M., Oberstein, P., 2017. Current and emerging therapies in metastatic pancreatic cancer. Clin. Cancer Res. 23, 1670–1678.
Meng, H., Wang, M.Y., Liu, H.Y., Liu, X.S., Situ, A., Wu, B., Ji, Z.X., Chang, C.H., Nel, A.E., 2016. Use of a lipid-coated mesoporous silica nanoparticle platform for synergistic gemcitabine and paclitaxel delivery to human pancreatic cancer in mice (vol 9, pg 3540, 2015). ACS Nano 10, 6416.
Moog, R., Burger, A.M., Brandl, M., Schuler, J., Schubert, R., Unger, C., Fiebig, H.H., Massing, U., 2002. Change in pharmacokinetic and pharmacodynamic behavior of gemcitabine in human tumor xenografts upon entrapment in vesicular phospholipid gels. Cancer Chemother. Pharmacol. 49, 356–366.
Park, S.H., Sung, J.H., Kim, E.J., Chung, N., 2015. Berberine induces apoptosis via ROS generation in PANC-1 and MIA-PaCa2 pancreatic cell lines. Braz. J. Med. Biol. Res. 48, 111–119.
Pasut, G., Canal, F., Dalla Via, L., Arpicco, S., Veronese, F.M., Schiavon, O., 2008. Antitumoral activity of PEG–gemcitabine prodrugs targeted by folic acid. J. Control. Release 127, 239–248.
Réjiba, S., Reddy, L.H., Bigand, C., Parmentier, C., Couvreur, P., Hajri, A., 2011. Squalenoyl gemcitabine nanomedicine overcomes the low efficacy of gemcitabine therapy in pancreatic cancer. Nanomedicine 7, 841–849.
Reddy, L.H., Couvreur, P., 2009. Squalene: a natural triterpene for use in disease management and therapy. Adv. Drug Deliv. Rev. 61, 1412–1426.
Reddy, L.H., Khoury, H., Paci, A., Deroussent, A., Ferreira, H., Dubernet, C., Declèves, X., Besnard, M., Chacun, H., Lepêtre-Mouelhi, S., Desmaële, D., Rousseau, B., Laugier, C., Cintrat, J.-C., Vassal, G., Couvreur, P., 2008. Squalenoylation favorably modifies the in vivo pharmacokinetics and biodistribution of gemcitabine in mice. Drug Metab. Dispos. 36, 1570–1577.
Reid, J.M., Qu, W.C., Safgren, S.L., Ames, M.M., Krailo, M.D., Seibel, N.L., Kuttesch, J., Holcenberg, J., 2004. Phase I trial and pharmacokinetics of gemcitabine in children with advanced solid tumors. J. Clin. Oncol. 22, 2445–2451.
Richards, K.E., Zeleniak, A.E., Fishel, M.L., Wu, J., Littlepage, L.E., Hill, R., 2017. Cancer-associated fibroblast exosomes regulate survival and proliferation of pancreatic cancer cells. Oncogene 36, 1770–1778.
Shi, C., Yu, H., Sun, D., Ma, L., Tang, Z., Xiao, Q., Chen, X., 2015. Cisplatin-loaded polymeric nanoparticles: characterization and potential exploitation for the treatment of non-small cell lung carcinoma. Acta Biomater. 18, 68–76.
Song, W., Tang, Z., Shen, N., Yu, H., Jia, Y., Zhang, D., Jiang, J., He, C., Tian, H., Chen, X., 2016a. Combining disulfiram and poly(L-glutamic acid)-cisplatin conjugates for combating cisplatin resistance. J. Control. Release 231, 94–102.
Song, W., Tang, Z., Zhang, D., Li, M., Gu, J., Chen, X., 2016b. A cooperative polymeric platform for tumor-targeted drug delivery. Chem. Sci. 7, 728–736.
Song, W., Tang, Z., Zhang, D., Wen, X., Lv, S., Liu, Z., Deng, M., Chen, X., 2016c. Solid tumor therapy using a cannon and pawn combination strategy. Theranostics 6, 1023–1030.
Vandana, M., Sahoo, S.K., 2010. Long circulation and cytotoxicity of PEGylated gemcitabine and its potential for the treatment of pancreatic cancer. Biomaterials 31, 9340–9356.
Yan, J., Zhang, D., Yu, H., Ma, L., Deng, M., Tang, Z., Zhang, X., 2017. Patupilone-loaded poly(L-glutamic acid)-graft-methoxy-poly(ethylene glycol) micelle for oncotherapy. J. Biomater. Sci. Polym. Ed. 28, 394–414.
Yang, E., Qian, W., Cao, Z., Wang, L., Bozeman, E.N., Ward, C., Yang, B., Selvaraj, P., Lipowska, M., Wang, Y.A., Mao, H., Yang, L., 2015. Theranostic nanoparticles carrying doxorubicin attenuate targeting ligand specific antibody responses following systemic delivery. Theranostics 5, 43–61.
Yu, H., Tang, Z., Li, M., Song, W., Zhang, D., Zhang, Y., Yang, Y., Sun, H., Deng, M., Chen, X., 2016. Cisplatin loaded poly(L-glutamic acid)-g-methoxy poly(ethylene glycol) complex nanoparticles for potential cancer therapy: preparation, in vitro and in vivo evaluation. J. Biomed. Nanotechnol. 12, 69–78.
Yu, H., Tang, Z., Zhang, D., Song, W., Zhang, Y., Yang, Y., Ahmad, Z., Chen, X., 2015. Pharmacokinetics, biodistribution and in vivo efficacy of cisplatin loaded poly(L-glutamic acid)-g-methoxy poly(ethylene glycol) complex nanoparticles for tumor therapy. J. Control. Release 205, 89–97.
Zhang, C.Y., Pan, D.Y., Li, J., Hu, J.N., Bains, A., Guys, N., Zhu, H.Y., Li, X.H., Luo, K., Gong, Q.Y., Gu, Z.W., 2017. Enzyme-responsive peptide dendrimer-gemcitabine conjugate as a controlled-release drug delivery vehicle with enhanced antitumor efficacy. Acta Biomater. 55, 153–162.